Supporting Information

ZIF-derived *in Situ* Nitrogen-Doped Porous Carbons as Efficient Metal-free Electrocatalysts for Oxygen Reduction Reaction

Peng Zhang[1], Fang Sun[1], Zhonghua Xiang[1], Zhigang Shen[1], Jimmy Yun[2,3], Dapeng Cao[1*]

[1] State Key Lab of Organic-Inorganic Composites, Beijing University of Chemical Technology, Beijing 100029, P.R. China

[2] School of Chemical Science and Engineering, The University of New South Wales, Sydney NSW 2052 Australia

[3] Changzhou Institute of Advanced Materials, Beijing University of Chemical Technology, Changzhou 213164, P.R. China

*Corresponding author. Email: caodp@mail.buct.edu.cn Tel:+8610-64443254

Experimental section

Preparation of ZIF-7: A solid mixture of $Zn(NO_3) \cdot 6H_2O$ (4.425g, 14.875mmol) and benzimidazole (H-PhIM) (1.25g, 10.575mmol) was dissolved in 375 mL DMF in a 500 mL sealed vial. The vial was heated to 130 ^oC in a programmable oven at a rate of 5 $^oC\ min^{-1}$, and held at this temperature for 48h, then cooled at a rate of 0.4 $^oC\ min^{-1}$. The crystal was soaked in 20 ml organic solvent chloroform three times (once a day). Colorless crystals were washed with DMF (50ml×3) and evacuated at 150 ^oC in vacuum for 10h. FT-IR : (KBr 4000-400cm^{-1}): 3437(br), 3066(w), 2927(w), 1673(s), 1611(w), 1472(s), 1384(m), 1306(m), 1286(m), 1244(s), 1203(w), 1182(m), 1121(m), 1084(m),

1007(m), 909(m), 780(m), 738(s), 646(m), 466(m), 424(m).

Characterization methods: Powder X-ray diffraction (PXRD) measurements were performed with D8 ADVANCE X-ray diffactometer (Cu Kα, 40Kv, 20Ma, λ =1.54178Å). Raman spectra were recorded on a LabRAM Aramis Raman Spectrometer (HORIBA Jobin Yvon). Thermogravimetric analysis (TGA) data were obtained on a DTG-60A (SHIMADZU) instrument, with a heating rate of 10 $^{\circ}$C min^{-1} under flowing Ar. FT-IR spectroscopy was performed on an AC-80MHZ (Bruker) instrument with the wave range of 4000-400 cm^{-1}. XPS data were obtained on a ThermoFisher ESCALAB 250 X-ray photoelectron spectroscopy equipped with twin anode Mg Ka X-ray source. Chemical composition was obtained by using element analysis (vario EL cube V2.0.1). The morphologies and structures of materials were examined by using SEM (Zeiss SUPRA 55), TEM (Tecnai $G^2$20) and HRTEM (JEOL JEM-2100). EDS measurements were performed on an EDS system (Oxford INCA Energy 350 ADD), which an accessory of SEM, by using Mn Kα radiation. Metal element content was determined by ICP (Shimadzu IPCPS-7500). N_2 adsorption/ desorption isotherms were measured at 77K with ASAP 2020 analyzer (Micromeritics, U.S.A). Before measurements, the samples were degassed in a vacuum at 300 $^{\circ}$C for at least 24h. The specific surface area (S_{BET}) was calculated by the Brunauer-Emmet-Teller (BET) method, and the total pore volume was estimated from the adsorbed amount at a relative pressure P/P_0 of 0.9997. The pore size distribution was evaluated by density functional theory (DFT).

Calculation of electron transfer number

Koutecky-Levich plots were analyzed at various electrode potentials. The slopes of the linear fitting were used to calculate the number of electrons transferred (n) on the basis of the Koutecky-Levich equations,[1] given by

$$\frac{1}{J} = \frac{1}{J_L} + \frac{1}{J_K} = \frac{1}{B\omega^{1/2}} + \frac{1}{J_K} \quad \textbf{(S1)}$$

$$B = 0.62nFC_0(D_0)^{2/3}\upsilon^{-1/6} \quad \textbf{(S2)}$$

$$J_K = nF\kappa C_0 \quad \textbf{(S3)}$$

where J is the measured current density, J_K and J_L are the kinetic- and diffusion-limiting current densities, ω is the angular velocity of the disk ($\omega = 2\pi N$, N is the linear rotation speed), n is the overall number of electrons transferred in oxygen reduction reaction, F is the Faraday constant ($F = 96485\ C\ mol^{-1}$), C_0 is the bulk concentration of O_2, υ is the kinematic viscosity of the electrolyte, and κ is the electron-transfer rate constant. In 0.1 M KOH, the values can be determined: $C_O = 1.2 \times 10^{-3} molL^{-1}$; $D_0 = 1.9 \times 10^{-5} cms^{-1}$; $\nu = 0.1 m^2 s^{-1}$.

The electron transfer number per O_2 and $\%HO_2^-$ were calculated from the RRDE measurement.

$$n = 4I_d/(I_d + I_r/N) \quad \textbf{(S4)}$$

$$\%HO_2^- = 200 \times \frac{I_r/N}{I_d + I_r/N} \quad \textbf{(S5)}$$

Here I_d and I_r is the disk current and ring current, respectively, and N is the current collection efficiency of Pt ring (N=0.37).

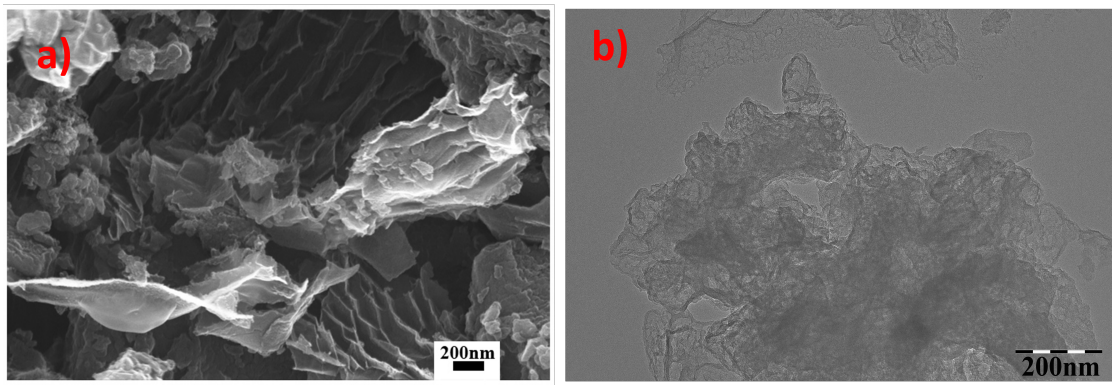

Fig.S1 a) SEM image and b) TEM image of as-prepared Carbon-S.

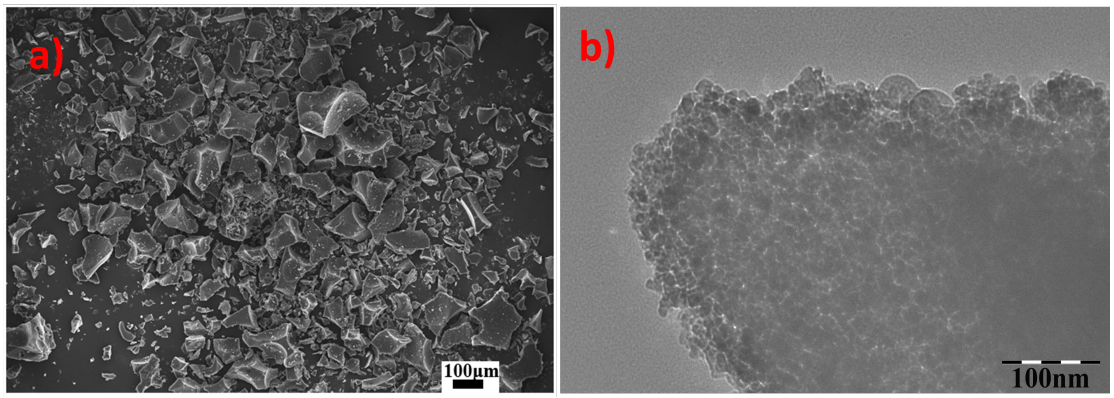

Fig.S2 a) SEM image and b) TEM image of as-prepared Carbon-G.

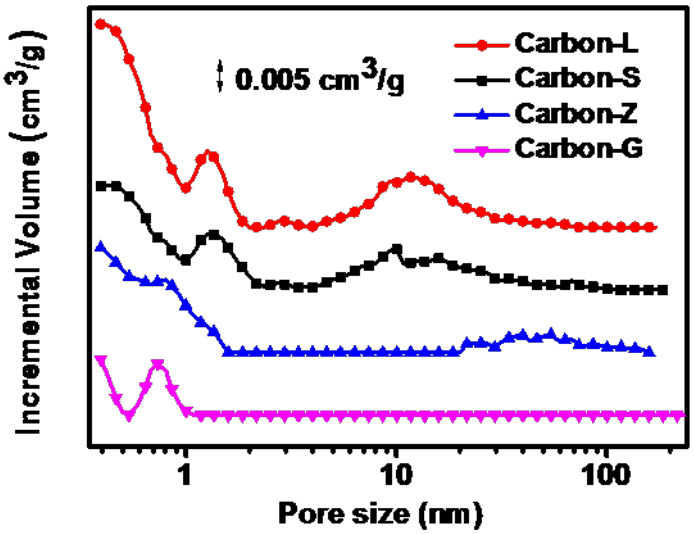

Fig.S3 DFT pore distribution of as-prepared Carbon-L (red line), Carbon-S (black line), Carbon-Z (blue line) and Carbon-G (magenta line).

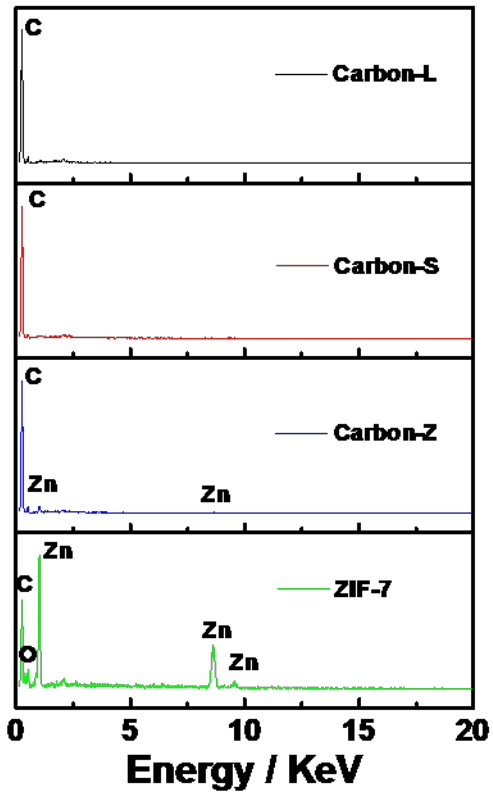

Fig.S4 EDS of as-prepared ZIF-7, Carbon-L, Carbon-S and Carbon-Z

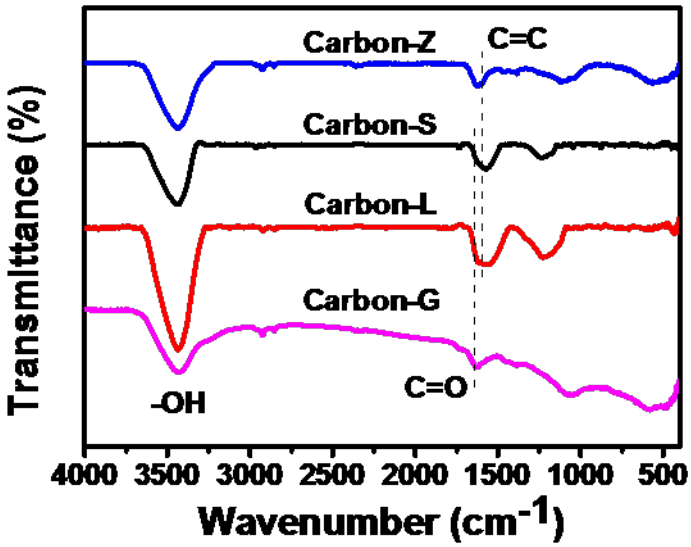

Fig.S5 FT-IR spectra of as-prepared Carbon-L (red line), Carbon-S (black line), Carbon-Z (blue line) and Carbon-G (magenta line).

Fig S5 shows the FT-IR spectra of four as-prepared porous carbons. The C=O of carboxyl group in three carbons with glucose and C=C of aromatic ring in ZIF-7 derived porous carbon are revealed by the band at 1640 cm^{-1} and 1580 cm^{-1}, respectively. They are overlapped to become a broad absorption peak.[2] The result of FT-IR reveals that there are abundant of -OH and C=O groups on the surface of Carbon-L and -S, those groups can remarkably improve the hydrophilicity and wettability at the surface of samples.[3] Meanwhile, it favors the preparation of electrode in this work.

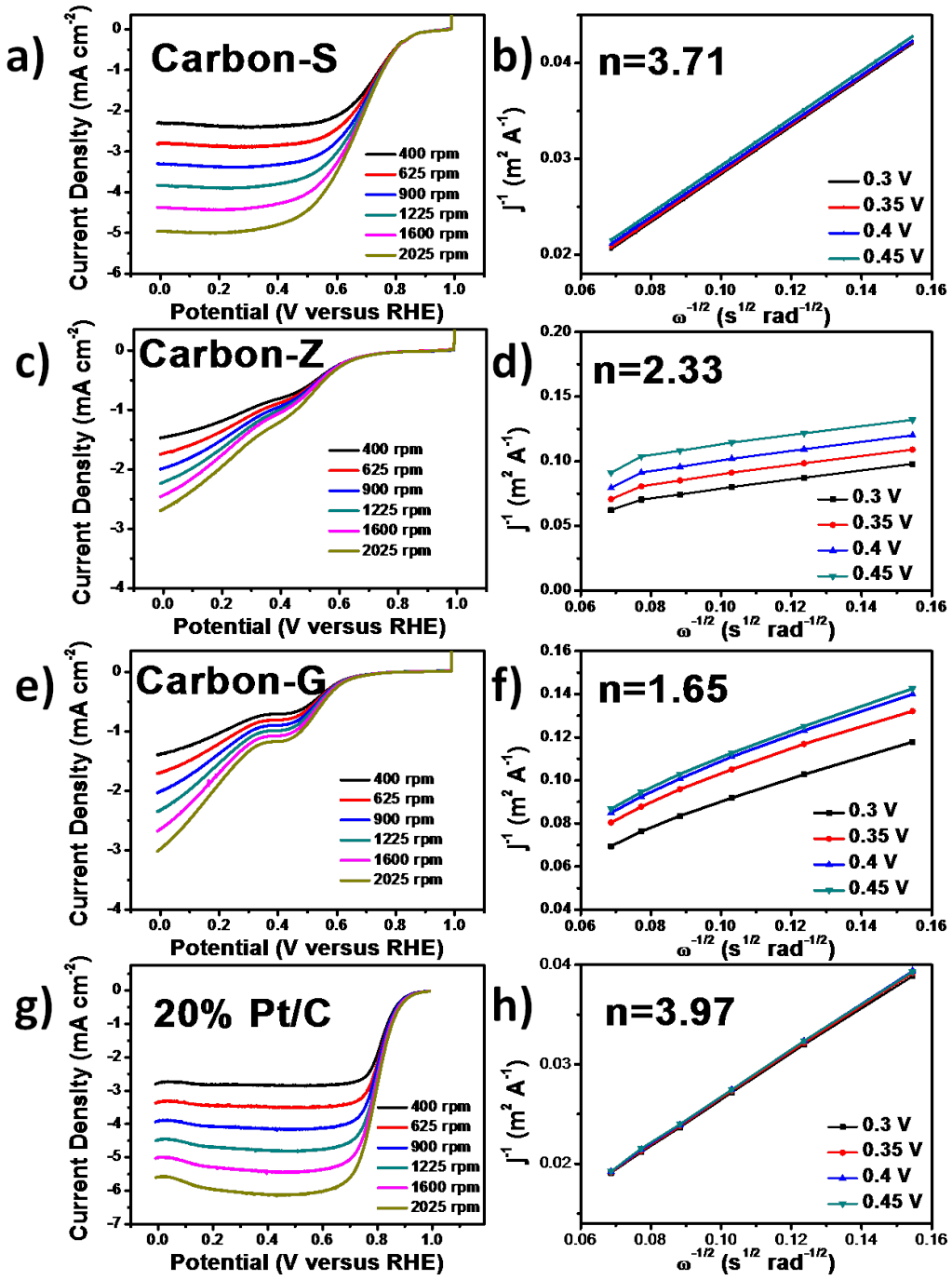

Fig.S6 Rotating-disk voltammograms of other catalysts in O_2-saturated 0.1 M KOH with a sweep rate of 5 mVs^{-1} at different rotation rates indicated and their corresponding Koutecky-Levich plots at different potentials. a), b) Carbon-S; c), d) Carbon-Z; e), f) Carbon-G； g), h) 20% Pt/C.

For the RRDE measurement, the catalyst ink was prepared by the same method as RDE. The 10μL of the suspension was transferred via a syringe on the surface of the RRDE (0.2472cm^2) to form a thin layer, which was subsequently dried slowly at room temperature to remove the residual solvent. The disk electrode was scanned cathodically at a rate of 5 mV s^{-1} and the ring potential was constant at 1.5V vs RHE. Disk current is shown on the lower half and ring current is shown on the upper half in Fig S7a. The n value of Carbon-L from the K-L equation (Eq S1-S3) is similar with the one calculated by the RRDE curve (Fig S7a and Eq S4). To further verify the ORR pathways on the Carbon-L and Carbon-Z, RRDE measurement was carried out to examine the amount of HO_2^- production during the ORR process. As shown in Fig S7b, the ring currents on the Carbon-L were lower than Carbon-Z, while the disk limiting currents were much higher than Carbon-Z, implying the lower HO_2^- production of Carbon-L. The addition of extra carbon source-glucose in the Carbon-L decreases HO_2^- production during ORRs, which leads to a significant improvement of operation performance in the fuel cells. Our results indicate that oxygen was reduced by the synergy between 2-electron and 4-electron routes in Carbon-L. The C-N active sites would be limited on account of low N content, which indicates that the two routes show contribution to the pathway of ORR in Carbon-L, but the four electron route mainly contributes to ORR (ca. about 70%) in Carbon-L.

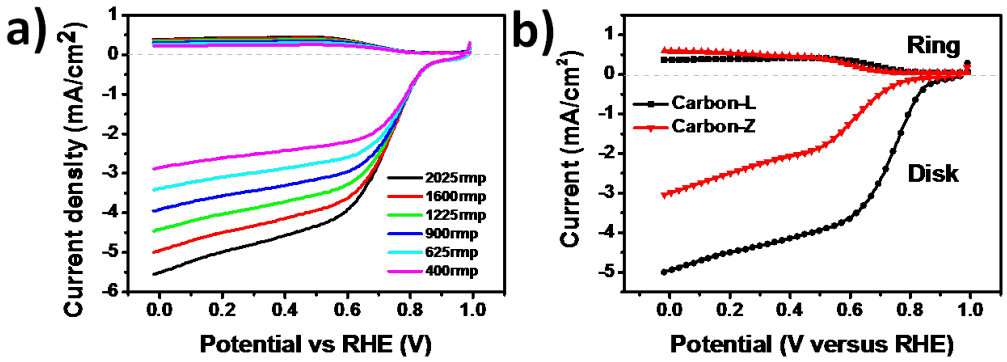

Fig.S7 a) Rotating ring-risk electrode voltammograms recorded with Carbon-L in O_2-saturated 0.1M KOH at different rotational speeds (from 400 to 2025 rmp). b) Comparative rotating ring-risk electrode voltammograms of different electrocatalysts at 1600rmp.

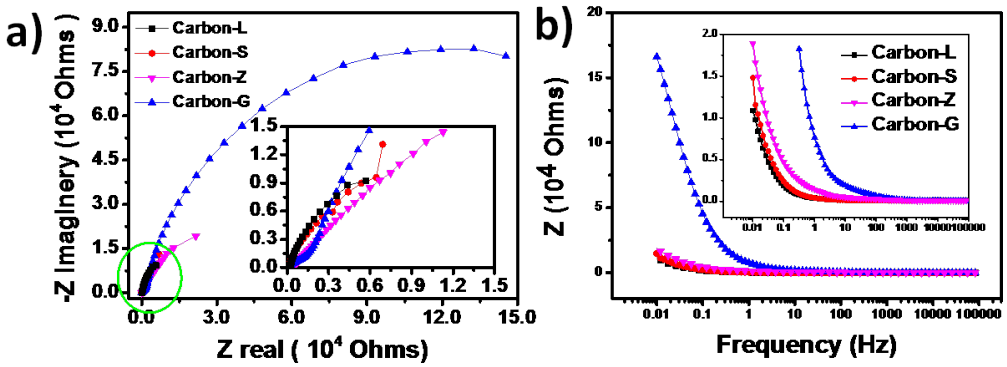

Fig.S8 (a) Nyquist and (b) Bode spectra of four synthesized porous carbons by applying a sine wave with amplitude of 5.0 mV over the frequency range from 100 kHz to 10 mHz.

We also test ZIF-derived carbons as electrocatalyst for ORR in acid medium. Except that electrolyte becomes 0.1M $HClO_4$ solution, other test conditions have not changed. All potentials were converted to the reversible hydrogen electrode (RHE) scale. As shown in Fig S9, a substantial positive shift in onset potential was observed. It is ~ 0.75 V for the Carbon-L, which is higher than Carbon-S (~0.71 V), Carbon-Z (~0.38 V) and Carbon-G (~0.27 V), indicating better ORR catalytic activity of Carbon-L than other carbons in this work. Remarkably, these values are comparable to the N-CNTs-750 electrode (~0.79 V) and commercial CNT electrode (~0.34 V) in

previous literature. [4] None of the polarization curves show a plateau for limited current density in the acidic solution for above all electrodes. Nevertheless, the onset potential for the Carbon-L electrode is more negative than that for the Pt/C electrode (~0.95 V) which is the evidence of the Carbon-L lower ORR activity than 20% Pt/C in acid medium. The worse electrocatalytic performance of the ZIF-derived carbons electrode resulted in no visible diffusion current plateau in the polarization curve, whereas the commercial 20% Pt/C electrode had a super diffusion current density. Definitely, the ZIF-derived carbons face more challenges for ORR in acid medium.

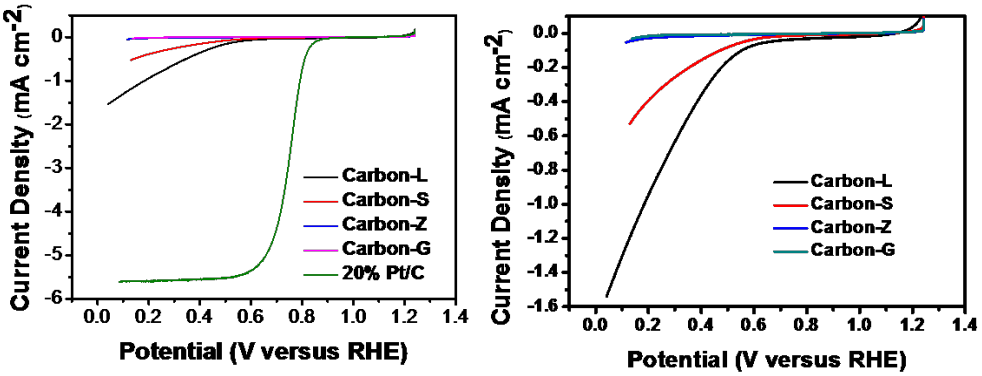

Fig.S9 Polarization curves of Carbon-L, Carbon-S, Carbon-Z, Carbon-G and commercial 20% Pt/C for oxygen reduction in O_2-saturated 0.1M $HClO_4$ at a rotation rate of 2025 rmp.

Table-S1 Elemental analysis of carbon, hydrogen and nitrogen for four carbons.

Sample	ZIF-7/g	Glucose/g	Temperature/℃	N%	C%	H%
Carbon-L	0.5	0.25	950	6.787	66.04	2.088
Carbon-S	0.5	0.25	950	3.426	76.18	1.195
Carbon-Z	0.5		950	7.331	80.34	0.8
Carbon-G		0.5	950		92.9	0.587

Table-S2 Summary of the electron transfer number, onset potential, half-wave potential and limiting current density for some other metal-free catalysts and MOF-derived electrocatalysts reported recently.

Sample	Synthetic methods	Electron transfer number	Onset potential [a]	Limiting current density	Half-wave potential	Refs
Carbon-L	Carbonizing ZIF-7/glucose composites (solid phase) at 950℃	3.33-3.93 at range of 0.15V-0.55V (3.68 at 0.3V)	0.86V	4.59 mA/cm^2	0.70V	Present work
Carbon-S	Carbonizing ZIF-7/glucose composites (liquid phase)at 950℃	3.47-3.9 at range of 0.15V-0.55V (3.71 at 0.4V)	0.84V	4.43 mA/cm^2	0.68V	Present work
Carbon-Z	Direct carbonization of ZIF-7 at 950℃	1.92-2.5 at range of 0.15V-0.55V	0.74V	2.51 mA/cm^2	0.32V	Present work
20% Pt/C	20 wt% Pt loading, Johnson Matthey, Pt/C	3.9-4.0 at range of 0.15V-0.55V	0.92V	4.87 mA/cm^2	0.80V	Present work
NPC-0	Pyrolysis of EDTA and melamine with KOH 700℃	3.23 at 0.3V	0.82V	4.16 mA/cm^2	0.73V	12
POF-C-1000	Nanocasting of PAF-6 and FA 1000℃	3.75 at -0.44V	-93.11mV vs Hg/HgO	5.24 mA/cm^2		1 7
POF-C-800	Nanocasting of PAF-6 and FA 800℃	3.53at -0.44V	-77.87mV vs Hg/HgO	4.21 mA/cm^2		17
PCF-DC-1000	Direct carbonization of PAF-6 1000℃	3.46 at -0.44V	-98.57mV vs Hg/HgO	3.85 mA/cm^2		17
PDI-600	Nanocasting technology of SBA-15 and PDI 600℃	1.8 at -0.35V	-0.23V vs Ag/AgCl (3M KCl)			59
PDI-750	Nanocasting technology of SBA-15 and PDI 750℃	2.56 at -0.35V	-0.15V vs Ag/AgCl (3M KCl)			59
PDI-900	Nanocasting technology of	3.89 at -0.35V	-0.13V vs Ag/AgCl			59

	SBA-15 and PDI 900℃		(3M KCl)			
Graphene-based nanomaterials	See refs 60	See refs 60				60
NCNC700	In situ MgO template method with pyridine precursor 700℃	3.26	-0.13V vs Ag/AgCl			61
NCNC700/900	NCNC700 was further annealed at 900℃	3.27	-0.13V vs Ag/AgCl			61
N-doped 3D GF	N-containing gel (GO and pyrrole) was freeze-dried and annealed at 1050℃	Approximately 3.7	-0.18V vs Ag/AgCl			62
FeIM700	FeIM pyrolysis at 700℃	3.7-3.81at range of 0V-0.7V	0.86V	4-5 mA/cm^2		50
FeIM800	FeIM pyrolysis at 800℃	3.59-3.78 at range of 0V-0.7V	0.86V			50
FeIM900	FeIM pyrolysis at 900℃	The worst catalyst in refs 50	0.82V			50
FeIM/ZIF-8	Ball-milling the FeIM and ZIF-8, pyrolysis at 1050℃	3.83-3.93 at range of 0V-0.7V	0.92V			50
1 activated at 750℃	Cobalt Imidazolate Framework as precursor activated at 750℃	3.2-3.5	0.83V in 0.1M $HClO_4$		0.68V	51

[a] All potentials were converted to the reversible hydrogen electrode (RHE) scale, unless otherwise stated.
All samples were tested in 0.1M KOH solution, unless otherwise stated.
The blank represent there are not stated in the original paper.

References

[1] A. J. Bard,L. R. Faulkner, *Electrochemical methods: fundamentals and applications*. Vol. 2. **1980**: Wiley New York.

[2] S. Mo, Z. Sun, X. Huang, W. Zou, J. Chen,D. Yuan, *Synth Met* **2012**, 162, 85.

[3] Q. Li, R. Jiang, Y. Dou, Z. Wu, T. Huang, D. Feng, J. Yang, A. Yu,D. Zhao, *Carbon* **2011**, 49, 1248.

[4] Z. Mo, S. Liao, Y. Zheng, Z. Fu, *Carbon* **2012**, 50,2620.